Chinese Chemical Letters 31 (2020) 1670–1673

Contents lists available at ScienceDirect

Chinese Chemical Letters

journal homepage: www.elsevier.com/locate/cclet

Communication

Solid-state template-free fabrication of uniform Mo_2C microflowers with lithium storage towards Li-ion batteries

Jinfeng Sun, Lingzhi Guo, Miaomiao Gao, Xuan Sun, Jinyang Zhang, Longwei Liang, Yang Liu, Linrui Hou, Changzhou Yuan*

School of Material Science & Engineering, University of Jinan, Ji'nan 250022, China

ARTICLE INFO

Article history:
Received 15 July 2019
Received in revised form 26 September 2019
Accepted 26 September 2019
Available online 26 September 2019

Keywords:
Mo_2C
Hierarchical microflowers
Li-ion batteries
Anode
Solid-state synthesis

ABSTRACT

Herein, we first report one-step synthesis of uniform Mo_2C microflowers (MCMFs) from low-cost precursors *via* industrialized solid-state strategy. With fine optimization in precursor ratio and pyrolysis temperatures, the as-fabricated MCMFs are assembled well with interconnected single-crystalline nanosheet subunits. More encouragingly, the resultant MCMFs are further highlighted as a competitive anode with robust and long-duration lithium-storage behaviors towards high-performance Li-ion batteries

With the upsurge demand of energy storage systems in industries from personal devices to automobiles, secondary batteries are increasingly required with both improved performance and lifetime [1,2]. During past decades, Li-ion batteries (LIBs) have drawn particular interest with their advantages of high energy densities and desirable cycling stability [3,4]. Electrode materials are the key factors in affecting performance of the LIBs. Graphite, as the widely used anode materials in LIBs, shows great advantages of low cost and high theoretical li-ion charge-storage performance. However, graphite usually suffer from low rate capability and poor cycle stability, which do not meet the requirements (fast charging) from commercial electronics and electric automobile. Recently, various electrode materials including TiO_2, Si, MoS_2 and Ge for LIBs have been developed, and exhibit good performance for Li-ion storage [5–8]. Nevertheless, there are still some significant issues to be solved, especially the large volume change during the charge/discharge process, which results in severely structure breakdown, electrode collapse and capacity fading [9,10]. Thus, fine exploration of anode materials with high capacity, high rate performance, and good cycling stability is still highly desirable for LIBs applications.

Recently, transition metal carbides (TMCs) including Ti_2C, Ti_3C_2, V_2C, Fe_3C and Nb_2C have attracted great attention for application in energy storage area [11–15]. Among these TMCs, molybdenum carbide (Mo_2C) is a favorable candidate for anode materials, due to its merits of inherent electrochemical properties, high electrical conductivities, and good chemical stability [16,17]. However, on one hand, the capacity properties of single phase Mo_2C is still unsatisfied and less recognized, on the other hand, the complex synthesis technologies greatly impede the extensive use of Mo_2C for anode materials [17–19]. Thus, rational structure design, and simple, effective synthetic strategies of Mo_2C with good energy storage performance are of great significance.

Herein, we report a one-step solid-state strategy for the synthesis of uniform Mo_2C microflowers (MCMFs) from low-cost starting materials of $(NH_4)_6Mo_7O_{24}{\cdot}4H_2O$ and sodium citrate. The optimized MCMFs are composed by interconnected single-crystalline nanosheets (NSs) building blocks. Furthermore, the MCMFs electrode is highly promising as an anode with remarkable Li-ion storage properties for high-performance LIBs.

$(NH_4)_6Mo_7O_{24}{\cdot}4H_2O$ (AR, Aladdin Chemicals, 0.5 g) and sodium citrate (AR, Aladdin Chemicals, 0.5 g) with a mass ratio of 1:1 were grinded in a mortar for several minutes. The obtained mixture was put into a ceramic boat and then transferred into tube furnace and annealed in Ar atmosphere at 800 °C for 1 h with a heating rate of 3 °C/min. After that, the obtained power (~0.46 g) was putted into 20 mL 1 mol/L HCl, and further stirred for 2 h. Then, the black precipitate (Mo_2C) was collected by filtration, washed thoroughly with distilled water, and dried in an oven at 80 °C. Finally, the resultant product was ~0.113 g. For comparison, sodium citrate/$(NH_4)_6Mo_7O_{24}{\cdot}4H_2O$ with different mass ratios or treated in different heat temperatures (600, 700, 900 and 1000 °C) were also carried out.

* Corresponding author.
E-mail addresses: mse_yuancz@ujn.edu.cn, ayuancz@163.com (C. Yuan).

https://doi.org/10.1016/j.cclet.2019.09.049

X-ray diffraction (XRD) patterns of the samples were recorded with a Shimadzu powder X-ray diffractometer at the 2θ range from 10° to 80° using Cu Kα radiation (λ = 0.15406 nm). Morphologies and structures of samples were investigated by using a field-emission scanning electron microscopy (FESEM) system (JEOL, model JSM-7600 F). Transmission electron microscopy (TEM), selected area electron diffraction (SAED) and high-resolution TEM (HRTEM) characterization were determined with a JEOL 2100 F.

The electrode slurry was prepared by mixing as-synthesized MCMFs, carbon black and polyvinylidene fluoride in an *N*-methyl-2-pyrrolidone solvent with a weight ratio of 90:5:5. Then the slurry was pasted onto a copper foil and dried in a vacuum oven at 110 °C. The mass loading was around 1.0 mg. The coin-type cells (CR2032) were used for testing. The coin-type cells were assembled in an argon-filled glove-box with both the moisture and oxygen levels less than 1 ppm by using lithium foil as the counter electrode and 1 mol/L $LiPF_6$ in ethylene carbonate/diethyl carbonate (1:1, w/w) as the electrolyte. Galvanostatic discharge/charge tests were performed using a LAND CT2001A test system at a voltage window of 0.01–3.0 V *versus* Li^+/Li. Cyclic voltammetry (CV) was performed at a scan rate of 0.2 mV/s with a CHI 660E electrochemical workstation.

MCMFs were synthesized by direct pyrolysis of the mixture of $(NH_4)_6Mo_7O_{24}{\cdot}4H_2O$ and sodium citrate in Ar atmosphere. In the controlled experiments, the effect of synthesis parameters, such as pyrolysis temperature and sodium citrate/$(NH_4)_6Mo_7O_{24}{\cdot}4H_2O$ ratio, upon specific structure and morphology of Mo_2C were investigated in detail. Fig. 1a shows XRD patterns of the samples fabricated at various temperatures ranging from 600 °C to 1000 °C with a sodium citrate/$(NH_4)_6Mo_7O_{24}{\cdot}4H_2O$ mass ratio of 1:1. XRD pattern of the sample obtained at 600 °C shows a broad peak at around 25°, which is typically associated to the amorphous organic-inorganic hybrids [20]. After pyrolysis at 700 °C, some weak diffraction peaks at 34.5° and 61.9° assigned to Mo_2C (JCPDS No. 35-0787) appear, indicating the formation of Mo_2C. As the pyrolysis temperature increases to 800 and 900 °C, both the produced samples clearly exhibit a set of characteristic peaks at 34.5°, 38.0°, 39.4°, 52.3°, 61.7°, 69.7°, 74.7° and 75.7°, which are rationally ascribed to the phase-pure Mo_2C. Further increasing the temperature up to 1000 °C, some new diffraction peaks arise around 40.6°, 58.6° and 73.7°, and can be attributed to the metallic Mo [21], suggesting the partial decomposition of Mo_2C at 1000 °C. FESEM image in Fig. 1b exhibits that MCMFs cannot be formed at 600 °C. As the temperature increases to 700 °C, small-sized nanoflowers become visible in the matrix (Fig. 1c), corresponding to the formation of Mo_2C (Fig. 1a). When the pyrolysis temperatures are up to 800 and 900 °C, MCMFs can be well formed (Figs. 1d and e). Nevertheless, the flower-like structure is somewhat collapsed at 1000 °C (Fig. 1f), which is associated with the partial decomposition of Mo_2C, as examined in Fig. 1a.

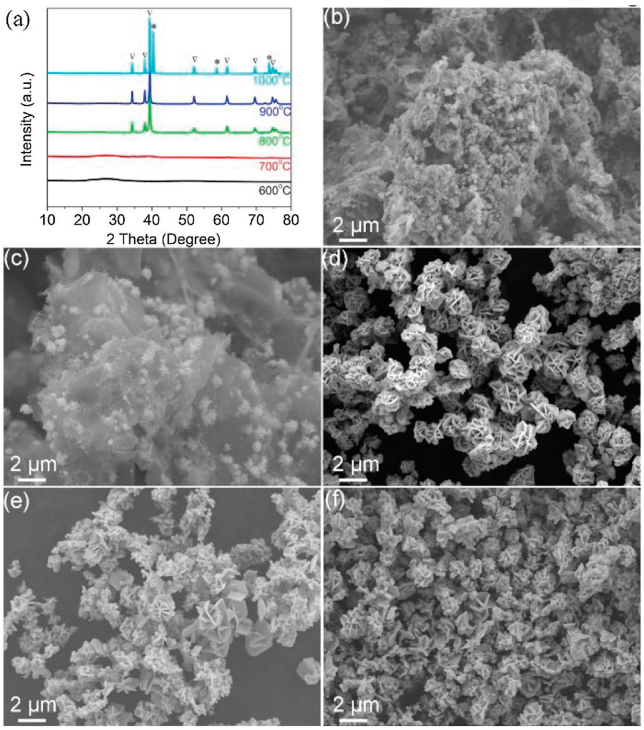

Fig. 1. (a) XRD patterns of the produced samples at the different temperatures, ▽-Mo_2C phase, *-metal Mo phase. FESEM images of the produced samples at the different temperatures: (b) 600, (c) 700, (d) 800, (e) 900 and (f) 1000 °C.

FESEM and XRD were used to characterize the structure and morphology of the samples synthesized with different sodium citrate/$(NH_4)_6Mo_7O_{24}{\cdot}4H_2O$ ratios at 800 °C, as presented in Fig. 2. It can be clearly seen that the less addition of $(NH_4)_6Mo_7O_{24}{\cdot}4H_2O$ (5:1) results in Mo_2C-carbon composite (Fig. 2a), while the surplus $(NH_4)_6Mo_7O_{24}{\cdot}4H_2O$ with sodium citrate/$(NH_4)_6Mo_7O_{24}{\cdot}4H_2O$ ratios lower than 1:3 leads to the formation of sheet-like MoO_3 (Figs. 2a, e and f). Mo_2C phase can be obtained as the sodium citrate/$(NH_4)_6Mo_7O_{24}{\cdot}4H_2O$ ratios are in the range of 1:2 to 2:1 (Fig. 2a). According to the above results, high-quality MCMFs can be achieved at 800 °C with a sodium citrate/$(NH_4)_6Mo_7O_{24}{\cdot}4H_2O$ ratio of 1:1. The optimized MCMFs shows the flower-like morphology with micro-size, which is constructed by interconnected NSs with a thickness of 50 nm on average, as shown in higher magnification FESEM image (Fig. 3a). The hierarchical microflower structure assembled by NSs subunits is further confirmed by TEM observation in Figs. 3b and c. A typical HRTEM image (Fig. 3d) illustrates the lattice fringes with a spacing of 0.23 nm, in good agreement with spacing of (101) of Mo_2C. Typical SAED pattern (the inset in Fig. 3d) shows a well-defined lattice, further indicating their single-crystalline characteristics of the NSs.

Furthermore, the Li-ion storage performance of the MCMFs was evaluated using a coin-type cell configuration with Li foil as the counter electrode. CV results of the initial cycles at a scan rate of 0.2 mV/s are collected, as shown in Fig. 4a. During the first cathodic process, the small cathodic peak at about 1.6 V and 1.2 V can be related to the insertion of a small amount of Li^+ into the layered structure of Mo_2C and the reduction of Mo^{4+} to the metallic phase, respectively [22]. The obvious cathodic peak at 0.7 V is attributed to the irreversible process of the formation of the solid electrolyte interphase film, which can be confirmed by its disappearance in the subsequent cycles [23]. In addition, the CV curves almost overlap with each other after the first CV sweep, indicating the excellent reversibility and stability of Mo_2C. Fig. 4b displays the galvanostatic discharge-charge plots of the MCMFs electrode at a rate of 0.05 A/g. The initial discharge and charge capacities of 273 and 180 mAh/g are obtained, respectively, corresponding to a Coulombic efficiency of 66%. The Li-ion storage capacity of the as-synthesized MCMFs is much higher than those of other Mo_2C anodes reported previously [16,18], which may be owing to the uniform microflower-like structure. The capacity loss in the first cycle can be attributed to the irreversible reactions by the formation of solid electrolyte interface layer, which is in good line with the CV results [24]. The followed discharge/charge curves of the 2nd cycle and 10th cycle seem to be overlapped, further demonstrating the good reversibility of MCMFs. The rate capability of Mo_2C (Fig. 4c) is also investigated within a wide current density range from 0.05-10 A/g. Remarkably, the MCMFs delivers specific capacities of 184, 182, 180, 166, 155 and

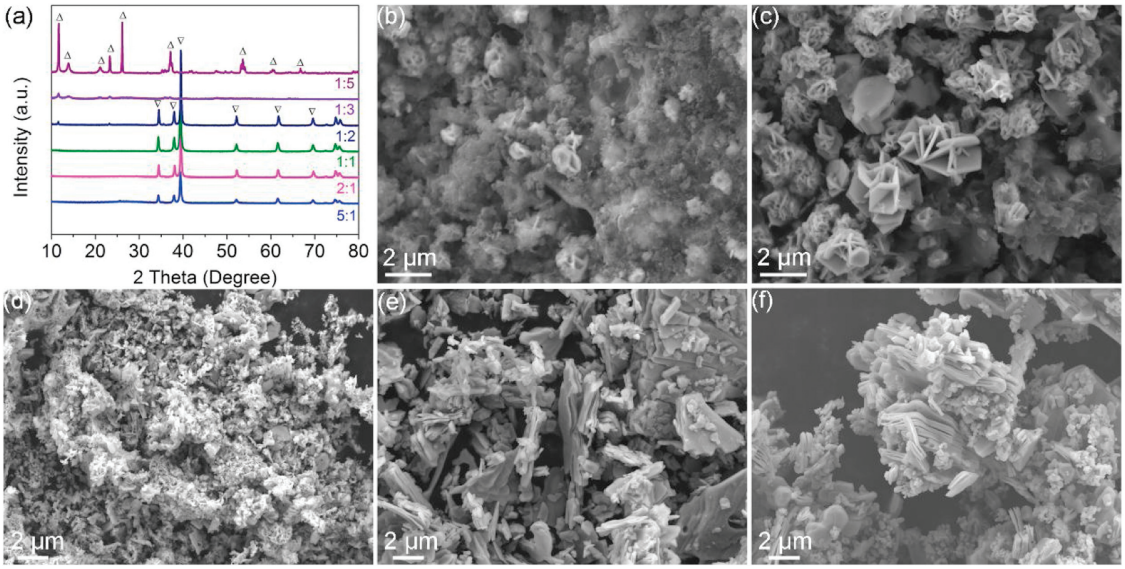

Fig. 2. (a) XRD patterns of the resulted samples at the different sodium citrate/ammonium molybdate mass ratios, Δ-MoO_3 phase, ∇-Mo_2C phase. (b–f) FESEM images of the produced samples at the different sodium citrate/ammonium molybdate mass ratios: (b) 5:1, (c) 2:1, (d) 1:2, (e) 1:3 and (f) 1:5.

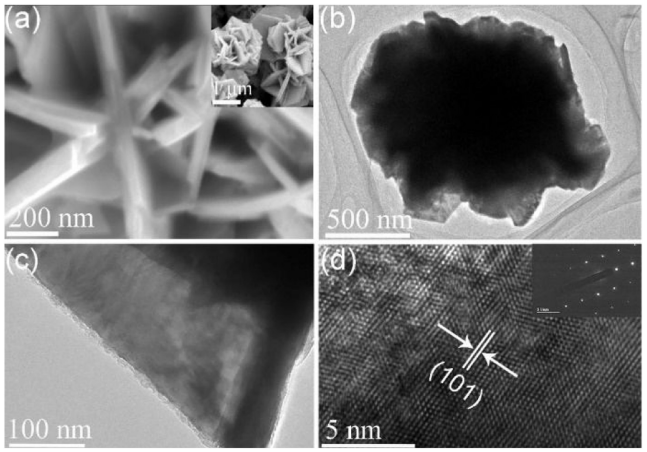

Fig. 3. (a) Higher magnification FESEM images of as-prepared MCMFs (the inset in panel a); (b, c) TEM images, (d) HRTEM image and corresponding SAED pattern (the inset in panel d) of a single Mo_2C nanosheet subunit.

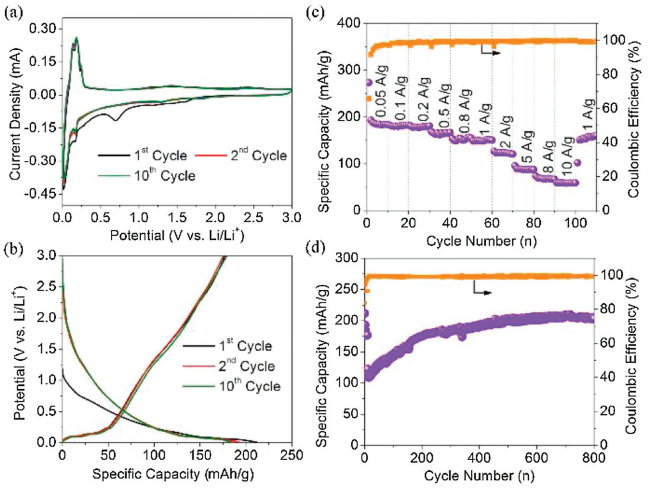

Fig. 4. Electrochemical performance of the MCMFs: (a) CV curves (0.2 mV/s); (b) Discharge/charge plots (0.05 A/g); (c) Rate capability evaluation with current range from 0.05 A/g to 10 A/g after the initial 10 cycles at 0.1 A/g; (d) Cycling stability at 1 A/g.

150 mAh/g (from 10^{th} cycle) at the current densities of 0.05, 0.1, 0.2, 0.5, 0.8 and 1 A/g, respectively, which is superior to most of the pure phase Mo_2C anode, and even comparable to those for MoO_2 [10,17,18,25]. More competitively, even at super high current rates of 5, 8 and 10 A/g, it still obtains 87.5, 67.1 and 59.1 mAh/g, respectively. The high rate capability of Mo_2C may be ascribed to its unique microflower-shape architecture assembled with single-crystalline NSs, which may facilitate the Li^+ uptake and release particularly at high rates [26,27]. In addition, the MCMFs electrode shows a long-duration cycling life, as illustrated in Fig. 4d. The capacities of Mo_2C show a slow increase in the first 400 cycles and stabilized in the following cycles, which can be explained by the gradual activation of the electrode material [16,27]. Appealingly, a capacity as high as about 200 mAh/g still can be maintained even after 800 consecutive cycles at a high rate of 1 A/g. Besides, the Coulombic efficiency is always close to 100% during long-term cycling.

In summary, we reported a one-step, low-cost method to synthesize the microflower-like Mo_2C through direct pyrolysis of a mixture of $(NH_4)_6Mo_7O_{24}{\cdot}4H_2O$ and sodium citrate. The effect of synthetic parameters on structures and morphologies of Mo_2C were systematically investigated. The high-quality MCMFs constructed by single-crystalline NSs blocks were obtained at 800 °C with an $(NH_4)_6Mo_7O_{24}{\cdot}4H_2O$/sodium citrate ratio of 1:1, and exhibited large reversible capacity and long-duration lithium-storage behaviors even at high rates as competitive anode for LIBs. Our findings will provide a new strategy for fabricating Mo_2C-based materials and hold great promise for more energy-related applications.

Declaration of competing interest

The authors declare that they have no known competing financial interests or personal relationships that could have appeared to influence the work reported in this paper.

Acknowledgments

The authors acknowledge the financial support from National Natural Science Foundation of China (Nos. 51772127, 51772131, 51802119), Taishan Scholars (No. ts201712050), Major Program of Shandong Province Natural Science Foundation (No. ZR2018ZB0317) and Collaborative Innovation Center of Technology and Equipment for Biological Diagnosis and Therapy in Universities of Shandong.

References

[1] R. Schmuch, R. Wagner, G. Hörpel, T. Placke, M. Winter, Nat. Energy 3 (2018) 267–278.
[2] W. Li, Q. Ning, X. Xi, et al., Adv. Mater. 31 (2019) 1804766.
[3] D. Liu, W. Li, Y. Zheng, et al., Adv. Mater. 30 (2018) 1706317.
[4] P. Zhang, Y. Liu, Y. Yan, et al., ACS Appl. Energy Mater. 1 (2018) 4814–4823.
[5] H. Xu, J. Chen, Y. Li, et al., Sci. Rep. 7 (2017) 2960.
[6] R. Wang, S. Wang, D. Jin, et al., Energy Storage Mater. 9 (2017) 195–205.
[7] Z. Yi, N. Lin, Y. Zhao, et al., Energy Storage Mater. 17 (2019) 93–100.
[8] R. Mo, D. Rooney, K. Sun, H.Y. Yang, Nat. Commun. 8 (2017) 13949.
[9] R. Wang, J. Lang, P. Zhang, Z. Lin, X. Yan, Adv. Funct. Mater. 25 (2015) 2270–2278.
[10] R. Wang, P. Liu, J. Lang, L. Zhang, X. Yan, Energy Storage Mater. 6 (2017) 53–60.
[11] Y. Huang, X. Lin, X. Zhang, et al., Electrochim. Acta 178 (2015) 468–475.
[12] D. Sun, M. Wang, Z. Li, et al., Electrochem. commun. 47 (2014) 80–83.
[13] J. Hu, B. Xu, C. Ouyang, S.A. Yang, Y. Yao, J. Phys. Chem. C 118 (2014) 24274–24281.
[14] J. Come, M. Naguib, P. Rozier, et al., J. Electrochem. Soc. 159 (2012) A1368–A1373.
[15] M. Naguib, J. Halim, J. Lu, et al., J. Am. Chem. Soc. 135 (2013) 15966–15969.
[16] X. Yang, Q. Li, H. Wang, et al., Chem. Eng. J. 337 (2018) 74–81.
[17] Q. Gao, X. Zhao, D. Zhao, M. Cao, Nanoscale 6 (2014) 6151–6157.
[18] H.J. Zhang, K.X. Wang, X.Y. Wu, et al., Adv. Funct. Mater. 24 (2014) 3399–3404.
[19] B. Wang, G. Wang, H. Wang, J. Mater. Chem. A Mater. Energy Sustain. 3 (2015) 17403–17411.
[20] Y. Leng, J. Li, C. Zhang, et al., J. Mater. Chem. A Mater. Energy Sustain. 5 (2017) 17580–17588.
[21] S.R. Vallance, S. Kingman, D.H. Gregory, Chem. Commun. (Camb.) (2007) 742–744.
[22] T. Stephenson, Z. Li, B. Olsenab, D. Mitlin, Energy Environ. Sci. 7 (2014) 209–231.
[23] Y. Zheng, T. Zhou, X. Zhao, et al., Adv. Mater. 29 (2017) 1700396.
[24] L. Shen, H. Lv, S. Chen, et al., Adv. Mater. 29 (2017) 1700142.
[25] Y. Zhu, S. Wang, Y. Zhong, et al., J. Power Sources 307 (2016) 552–560.
[26] S.H. Lee, S.H. Yu, J.E. Lee, et al., Nano Lett. 13 (2013) 4249–4256.
[27] C. Yan, C. Lv, Y. Zhu, et al., Adv. Mater. 29 (2017) 1703909.